AD-A032 875 GEORGIA INST OF TECH ATLANTA SCHOOL OF AEROSPACE ENG--ETC F/G 20/1
AUDIBLE AND ULTRASONIC ACOUSTIC EMISSIONS FROM COMPOSITE SOLID --ETC(U)
SEP 76 W A BELL, J I CRAIG, W C STRAHLE AF-AFOSR-2805-75
UNCLASSIFIED AFOSR-TR-76-1193 NL

1 OF 1
AD A032875

END
DATE FILMED
1 -77

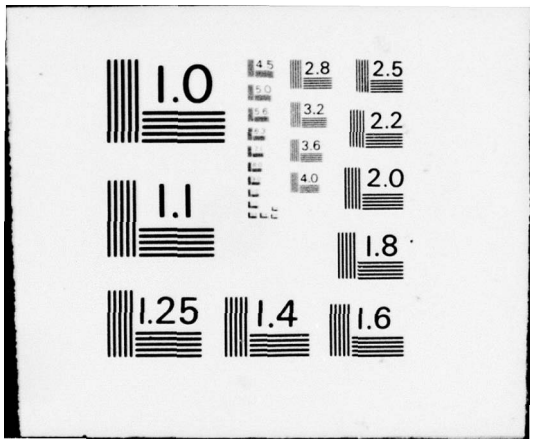
1.0
1.1
1.25
1.4
1.6
1.8
2.0
2.2
2.5
2.8
3.2
3.6
4.0
4.5
5.0

AFOSR - TR - 76 - 1193

AFOSR Interim Scientific Report

AFOSR-TR-

(11)

Audible and Ultrasonic Acoustic Emissions fron Composite Solid Propellants

prepared for

Air Force Office of Scientific Research
Aerospace Sciences Directorate

by

William A. Bell
James I. Craig
Warren C. Strahle

School of Aerospace Engineering
Georgia Institute of Technology
Atlanta, Georgia 30332

Grant No. AFOSR-75-2805

September 1976

UNCLASSIFIED

SECURITY CLASSIFICATION OF THIS PAGE (When Data Entered)

REPORT DOCUMENTATION PAGE

READ INSTRUCTIONS BEFORE COMPLETING FORM

1. REPORT NUMBER: AFOSR-TR-76-1193
2. GOVT ACCESSION NO.
3. RECIPIENT'S CATALOG NUMBER

4. TITLE (and Subtitle): AUDIBLE AND ULTRASONIC ACOUSTIC EMISSIONS FROM COMPOSITE SOLID PROPELLANTS.

5. TYPE OF REPORT & PERIOD COVERED: Interim scientific rept. July 1975-September 1976, INTERIM

6. PERFORMING ORG. REPORT NUMBER

7. AUTHOR(s): WILLIAM A. BELL, JAMES I. CRAIG, WARREN C. STRAHLE

8. CONTRACT OR GRANT NUMBER(s): AF-AFOSR 75-2805-75

9. PERFORMING ORGANIZATION NAME AND ADDRESS
GEORGIA INSTITUTE OF TECHNOLOGY
SCHOOL OF AEROSPACE ENGINEERING
ATLANTA, GEORGIA 30332

10. PROGRAM ELEMENT, PROJECT, TASK AREA & WORK UNIT NUMBERS
681308
9711-01
61102F

11. CONTROLLING OFFICE NAME AND ADDRESS
AIR FORCE OFFICE OF SCIENTIFIC RESEARCH/NA
BLDG 410
BOLLING AIR FORCE BASE, D C 20332

12. REPORT DATE: Sep 1976

13. NUMBER OF PAGES: 35

14. MONITORING AGENCY NAME & ADDRESS (if different from Controlling Office): 37p.

15. SECURITY CLASS. (of this report): UNCLASSIFIED

15a. DECLASSIFICATION/DOWNGRADING SCHEDULE

16. DISTRIBUTION STATEMENT (of this Report)

Approved for public release; distribution unlimited.

17. DISTRIBUTION STATEMENT (of the abstract entered in Block 20, if different from Report)

18. SUPPLEMENTARY NOTES

19. KEY WORDS (Continue on reverse side if necessary and identify by block number)
ULTRASONICS
NOISE
SOLID PROPELLANT COMBUSTION
ACOUSTIC EMISSIONS

20. ABSTRACT (Continue on reverse side if necessary and identify by block number)

Audible and ultrasonic acoustic waves are generated during deflagration of composite solid propellants. The audible waves can be sensed by microphones while special high frequency pressure transducers are required to measure the ultrasonic signals. These acoustic emissions have a potential use both as diagnostics of the combustion and as a means for the study of fundamental burning processes. To date a family of composite HTPB-AP propellants have been tested. Results which show the effects of pressure level, atmosphere in which burned, AP particle size, aluminum addition, and aluminum coating are presented and discussed.

LB

DD FORM 1 JAN 73 1473 EDITION OF 1 NOV 65 IS OBSOLETE

UNCLASSIFIED

403914

Abstract

Audible and ultrasonic acoustic waves are generated during deflagration of composite solid propellants. The audible waves can be sensed by microphones while special high frequency pressure transducers are required to measure the ultrasonic signals. These acoustic emissions have a potential use both as diagnostics of the combustion and as a means for the study of fundamental burning processes. To date a family of composite HTPB-AP propellants have been tested. Results which show the effects of pressure level, atmosphere in which burned, AP particle size, aluminum addition, and aluminum coating are presented and discussed.

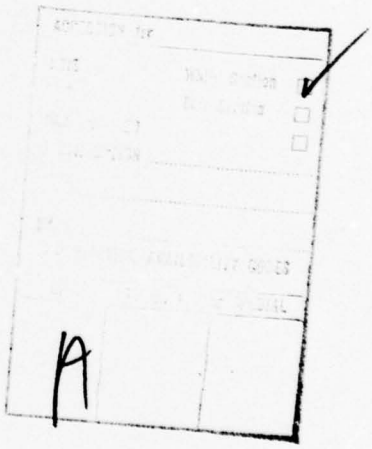

Table of Contents

I. Introduction

Deflagration of composite solid propellants is a complex, unsteady process involving a heterogeneous material. Consequently, experimental studies of the combustion dynamics are difficult to perform because of both the inaccessability of the process and the relatively small scale of heterogeneities. Average or integrated properties, such as the burn rate or the characteristic acoustic impedances of the propellant surface, have been measured during deflagration; but the details of the combustion processes must generally be studied by microscopic examination of the quenched propellant surface. Recent studies have been made[1,2] which relate ultrasonic acoustic emissions to the details of the combustion process.

This investigation is concerned with the use of audible and ultrasonic acoustic waves generated during deflagration to assist in the study of the combustion dynamics. These emissions are a direct result of unsteadiness caused by the heterogeneity of the propellant, and their measurement exemplifies the use of acoustic analysis in "turbulence" diagnostics. This technique consists of analyzing the frequency spectra of the noise produced by the deflagrating solid propellant and relating spectral characteristics to specific combustion processes. Deduced free-field audible emission measurements were taken and cover a range of frequencies from 40 Hz to 10 kHz. Ultrasonic emissions were also measured and reliable data were obtained from 50 kHz to 300 kHz. The acoustic fields for a family of AP-HPTB composite propellants, including coated and uncoated aluminized as well as nonaluminized formulations, were analyzed. The AP particle sizes range from 0.5 to 400 microns, and the propellants were burned in air, CO_2, and N_2 at pressures from 10 to 30 Atm.

The effects of mean pressure, pressurization gas, AP particle size, aluminum addition, and aluminum coating are discussed. Theories are presented which explain low frequency behavior (0-300Hz) although the high frequency behavior, which accounts for most of the noise, is open to interpretation.

II. Experiment

The deflagration tube shown in Fig. 1 is used in this study and can operate at pressures up to 70 Atm. The tube consists of a stainless steel pipe 162.5 cm in length with a nominal ID of 10.16 cm and an O.D. of 15.25 cm. The tube dimensions were originally chosen to satisfy the following criteria: (1) the volume of the tube should be sufficient so that the mean pressure level does not increase more than 10% during a run for the propellant strands used in this study; (2) the tube should be long enough to ensure fully developed wave propagation at some axial distance sufficiently far from the propellant; and (3) the first transverse mode should have a frequency higher than that expected for the peak of the sound power spectrum emitted from the propellants. Recent developments in accounting for three-dimensional waves in the tube have made it possible to relax this last assumption. Provisions are made along the tube for pressurization and evacuation. The gases used in this study were N_2, air and CO_2.

At one end of the tube, the solid propellant sample is held with epoxy to an aluminum sample holder which is bolted to a steel endplate 2.5 cm thick. Behind this endplate directly opposite the sample, a Dunegan-Endevco Model D 9201 flat response transducer is mounted to measure the ultrasonic acoustic emissions. To ensure a clean transmission path for the signal, high-vacuum grease is used between the

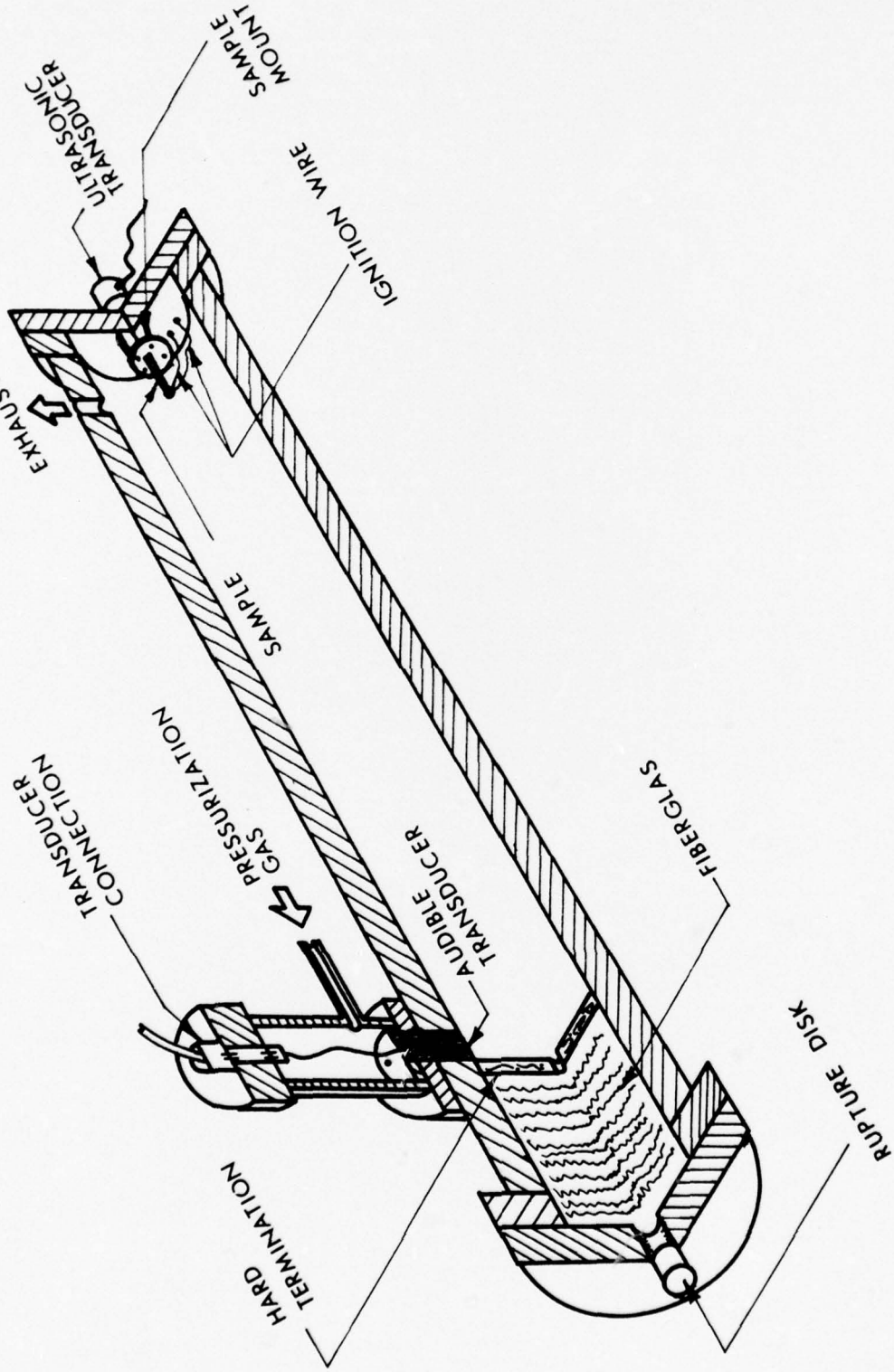

FIGURE 1. SCHEMATIC OF DEFLAGRATION TUBE.

sample holder and the endplate and a coupling grease is employed at the transducer-endplate interface. Electrical connections on the endplate allow the ignition wire to be joined to the igniter.

At the other end of the tube is another endplate to which a rupture disc is attached, as shown in Fig. 1. Twenty cm away along the axis of the tube a termination disc is located with a vent hole in the center. Fiberglass is placed between the disc and endplate to prevent acoustic feedback. The cavity between the disc and the endplate acts as a Helmholtz resonator and reduces the high amplitudes which occur at the lower resonant frequencies of the tube so that better signal resolution can be achieved at the higher frequencies. Directly in front of the termination disc, the audible transducer - a BBN Model 376A piezoelectric sensor - is located. To minimize pressure differentials across the transducer, it is surrounded by a cylindrical cavity which is coupled to the deflagration tube.

As shown in Fig. 2, the signals from both the audible and ultrasonic transducers are amplified, filtered, and then recorded on an Ampex 14-channel tape recorder at a speed of 60 inches per second. The FM mode is used for the audible signals and the AM mode is selected for the ultrasonic signals. The upper limit of response for the tape recorder is 300 kHz. The signals are then played back at a reduced rate for digital Fourier analysis using an HP5451A Fourier Analyzer. Typical results are presented in Fig. 3 for the audible signal and consist of the power spectrum over a specified frequency range. The narrow peaks occur at the resonant frequencies of the tube. A theory has been developed to deduce the equivalent free field spectra from the tube spectra and is presented in the next section.

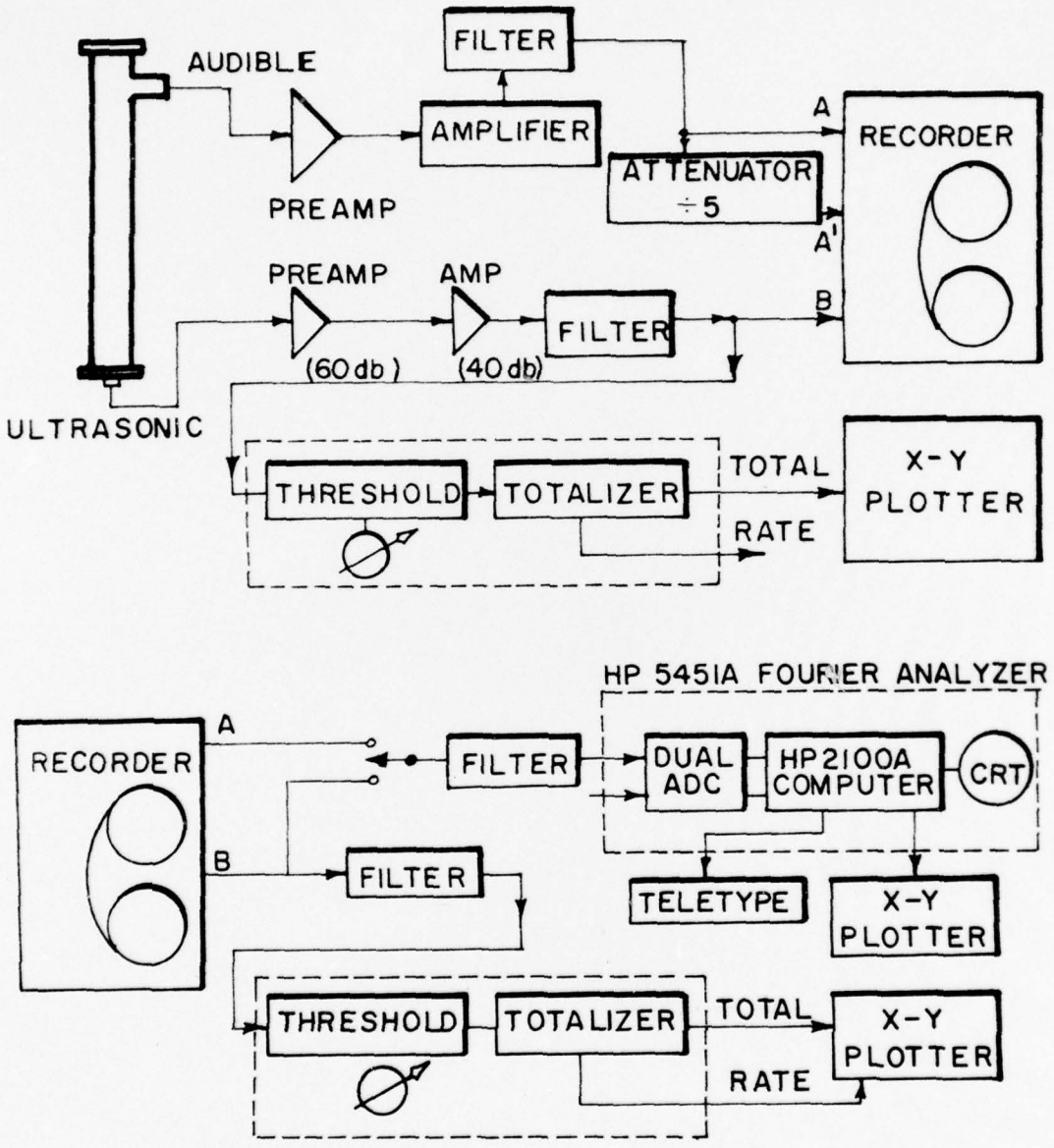

FIGURE 2. DATA ACQUISITION AND ANALYSIS SCHEMATIC

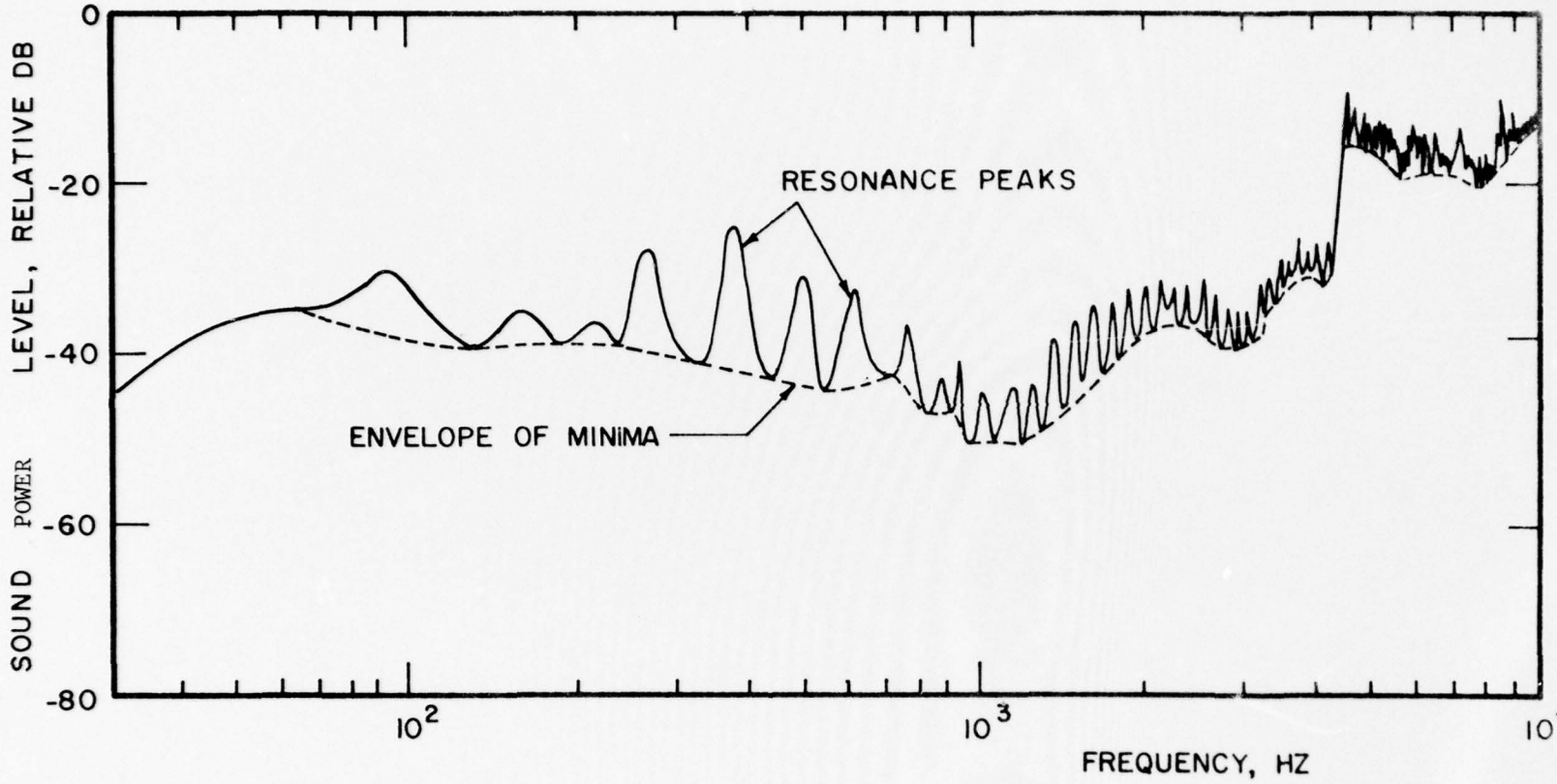

FIGURE 3. RAW SPECTRUM FOR NT-2 BURNING IN NITROGEN AT 300 PSIA.

III. Theory

Audible

The theoretical investigation for the audible emissions include (1) calculation of the equivalent free field sound power level and spectrum from the deflagration tube measurements, (2) determination of the mass flow noise efficiency $P/\dot{m}$, and (3) formulation of scaling laws to assist in combustion analysis.

The overall measured sound pressure level and the spectrum, of course, depend upon the acoustic properties of the tube. As shown in Fig. 3, resonances will appear at the natural mode frequencies of the tube. The data would be useless in an engineering sense if they could only be interpreted as unique to this configuration. What are actually desired are the sound power and spectral characteristics of the propellant in the absence of reflecting surfaces, i.e., the characteristics that would be obtained if the propellant were burning in a pressurized anechoic chamber. If this information can be extracted then theoretical acoustics may be employed to determine the acoustical behavior of any rocket chamber in which the propellant might be placed.

Over the frequency range from 0 to 2000 Hz, plane waves exist in the tube and the theory developed in Ref. 3 can be used to obtain the equivalent free field spectrum and sound power. Above 2000 Hz, however, three-dimensional modes are present, so the one-dimensional theory must be extended.

Since the Mach number is small, flow effects can be neglected. Also, any feedback of the reflected wave from the disc termination can be neglected.[3] The governing equation for acoustics of the tube are given by

the Helmholtz equation[4]

$$\nabla^2 p_\omega + k^2 p_\omega = 0 \qquad (1)$$

In the present experiment, cylindrical coordinates are applicable and the tube walls are assumed rigid ($\frac{\partial p_\omega}{\partial r} = 0$). The boundary conditions at the ends of the tube are

$$\frac{\partial p_\omega}{\partial x} = A_\omega \, \delta(r) \qquad (2)$$

at the propellant's end where the sample is assumed to be a point source of axial velocity fluctuations located at r = 0, and

$$\frac{\partial p_\omega}{\partial x} - i k y_\ell \, p_\omega = 0 \qquad (3)$$

at the other end of the tube. At frequencies greater that about 100 Hz, the admittance y_ℓ is about the same as a short nozzle.[3] A solution of the form

$$p_\omega = \sum_{m,n=0}^{\infty} (A_+ e^{-ik_{mn}x} + A_- e^{ik_{mn}x}) J_m \left(\frac{S_{mn} r}{a} \right) \cos m\theta \qquad (4)$$

is assumed. Applying Eq. (2) gives

$$(-A_+ + A_-) \sum_{m,n=0}^{\infty} \left[ik_{mn} J_m \left(S_{mn} \frac{r}{a} \right) \cos m\theta \right] = A_\omega \, \delta(r)$$

Multiplying both sides of this expression by $J_\mu (S_{\mu\eta} r)$ and integrating over the endplate area gives

$$- A_+ + A_- = \frac{A_\omega}{i \sum_{\substack{n=0 \\ k_{on} < k}} \pi a^2 k_{on} \, J_o{}^2 \left(\frac{S_{on}}{a} \right)}$$

With the propellant located at r=0, only radial modes exist in the tube.[4] For tangential modes (m > 0) a pressure node is located at the

tube's center. But since the propellant is placed at r=0, a pressure antinode exists at the center which means that the conditions for the formation of tangential modes cannot be maintained.

In the last expression the series in the denominator is restricted to values of k greater than the cutoff frequency k_{on}. At frequencies below the cutoff values the radial modes decay rapidly with axial distance.

Applying Eq. (3), solving for A_+ and A_-, and substituting the expressions into Eq. (4) gives, for the transducer located at x=ℓ, r=a:

$$p\, p_\omega^* = \frac{A_\omega A_\omega^*}{\sum_{n=0}^{k_{on}<k} \left[\pi a^2 J_o\left(\frac{S_{on}}{a}\right)\right]^2 (k^2 |y_\ell|^2 \cos^2 k_{on}\ell + k_{on}^2 \sin^2 k_{on}\ell - 2 k y_i k_{on} \sin k_{on}\ell \cos k_{on}\ell)} \tag{5}$$

For a flame burning in the free field,[5]

$$p_\omega\, p_\omega^* = \frac{A_\omega A_\omega^*}{(\pi R)^2} \tag{6}$$

so that measurement of $A_\omega A_\omega^*$ from $p_\omega\, p_\omega^*$ in the tube directly using Eq. (5) gives information about the free field source behavior through Eq. (6). In addition, once $A_\omega\, A_\omega^*$ is determined it can be used as a boundary condition similar to Eq. (2) in any generally shaped combustion chamber.

To facilitate the computation of $A_\omega\, A_\omega^*$ from typical spectral data shown in Fig. 3, the following observations are noted in Eq. (5). If $y_i = 0$, then at the minimum points of the spectrum where $\sin k_{on}\ell = 1$,

$$p_\omega p_\omega^*)_{min} = \frac{A_\omega A_\omega^*}{\sum_{n=0}^{k_{on}<k} \left[\pi a^2 k_{on} J_o\left(\frac{S_{on}}{a}\right) \right]^2} \qquad (7)$$

Preliminary tests of the tube using a known sound source indicate that $y_i = 0$ for the termination disc at frequencies above 100 Hz. Below this frequency, the peak-to-trough height in Fig. 3 is about 10 db which indicates that $|y_\ell|$ is small. Thus, Eq. (5) is apparently a good approximation below 100 Hz as long as $\sin k_{on} \ell$ does not approach zero. Equation (7) implies that $A_\omega A_\omega^*$ can be measured directly from the minima of the tube spectra if $A_\omega A_\omega^*$ does not vary appreciably with frequency.

Once $A_\omega A_\omega^*$ is determined, two important propellant combustion characteristics can be obtained. The first is the shape of the free field spectrum from which deflagration behavior diagnostics can be deduced. Secondly, the acoustic power generation capability can be obtained from the relation

$$P = \frac{1}{4\pi} \int_{-\infty}^{\infty} \frac{2\pi}{t_o} A_\omega A_\omega^* \, d\omega \qquad (8)$$

By dividing the power P by the mass flow rate $\dot{m}$ computed from the measured burn rates, the mass flow noise efficiency can be obtained.

Combustion noise is basically produced by a velocity source, as assumed in Eq. (2), in other flame types[6] and there is no reason to suspect this is not the case here. Velocity roughness downstream of the flame may easily be caused by the heterogeneous character of the propellant. Following the development of Ref. 6 the equivalent open flame acoustic power may be expected to scale like

$$P \propto \frac{\bar{\rho}}{\bar{c}} A_p \left(\frac{\rho_s r}{\bar{\rho}} \right)^4 \qquad (9)$$

A test of this relation was made with the current propellants. That is, the power should scale directly with the propellant surface area A_p and, for the same propellant energetics ($\bar{\rho}$), the acoustic power should increase as the burn rate r to the fourth power. Again, following the lead of Ref. 6 the majority of the frequency content of the noise should be located near

$$f \propto (\rho_s r/\bar{\rho})/\ell_e \tag{10}$$

According to Eq. (10) if the mean granularity (particle size) ℓ_e is reduced, the frequency content of the noise should rise, and an increase in the burn rate for a fixed $\bar{\rho}$ should increase the frequency. In the current tests $\bar{\rho}$ and ρ_s have been held constant so the only variables investigated were propellant burn rate, burn area and particle size.

Ultrasonic Acoustic Emissions

Acoustic emissions can be brcadly defined as stress wave emissions propagating within a solid material in response to some type of loading. The emission levels are generally well below those associated with audible disturbances and for many materials are on the order of microbars.

The investigation of deflagrating solid propellants by study of the ultrasonic emission spectrum must, at present, be general in nature for basically three reasons. First, the general meaning of the spectrum has yet to be formulated in any area of study. For solid propellants the inability to precisely define the propellant acoustical properties and its inhomogeneity greatly complicate data interpretation. Secondly, a suitable acoustic emission transducer with adequate bandwidth and relatively uniform response above 100 kHz is unavailable. Finally, frequency dependent attenuation of the waves caused by their dispersive propagation

through the propellant and signal distortion produced by reflection at interfaces complicates data interpretation.

In the present investigation, studies of propellants with greatly different properties were tested to determine if any general trends can be noticed. To account for the lack of flat transducer response at the frequencies tested, a transducer calibration spectrum was used to correct the measured spectra. At the outset, a calibration curve determined by the manufacturer using an impulsive acoustic emission technique (Ref. 7) was used for this purpose. This curve shows a smooth behavior from about 50 kHz to the 300 kHz limit of the tape recorder; however, closer examination and discussion with the manufacturer revealed that the "points" at 50 kHz spacing are simply rms level measurements using a tuned voltmeter and therefore represent overaged output over a band centered every 50 kHz.

In order to provide finer spectrum detail, an alternate qualitative calibration technique was used. Instead of measuring the transducer output for a known input stress wave (pressure), the electrical impedance of the transducer was measured over the frequency range of interest. Piezoelectric material such as that used for the present transducer generally exhibits a reversible behavior, that is, a charge is produced on certain crystal faces in response to an applied stress while a strain state can be produced in the crystal in response to an applied electric field (Ref.8). The relationship is linear, but due to anisotropy may involve extensive cross-coupling (e.g., uniaxial stress may produce charge on several crystal faces). In acoustic emission transducers, the output is measured as a charge on two parallel

element faces produced in response to an applied stress field, Smaller charges are produced on other faces at the same time, but are not detected. Consequently, when electrically driven in order to measure the impedance, the transducer element will vibrate in a manner that is similar to that when subjected to an incident stress wave. Since voltages (fields) are applied to only one pair of faces, a unique inverse to the input condition is not achieved. Ceramic elements, such as are used for most transducers exhibit a strong piezoelectric effect in the poled direction with much smaller cross-coupling effects so that the transducer's driven electrical impedance will generally show a strong qualitative similarity to an actual stress wave calibration. This has been born out in tests to determine the effect of transducer coupling mechanisms on the calibration (9).

In the present work, this electrical technique was used to obtain finer qualitative calibration data than available from the transducer maker. The electrical impedance was measured for the as-mounted configuration and quantitatively matched at the peak response (near 100 kHz) to the absolute calibration wave furnished. The most notable difference was the presence of several small (1-3 dB) peaks near 180 kHz and above 300 kHz. Rolloff at 100 kHz for the "impulse" calibration reflects the rolloff of the preamp used by the manufacturer in this test.

Not only is the transducer spectral calibration subject to question, but as noted earlier, due to essentially intractable nonhomogeneities and geometric irregularities in the transmission media, the received signal may bear little resemblence to the pressure wave produced at the

emission source. Three mechanisms can be immediately noted:

(a) material dispersion in the viscoelastic, heterogeneous propellant

(b) geometric dispersion for a stress wave propagating in a prismatic bar

(c) attenuation due to acoustic impedance mismatch at material interfaces in the transmission path.

The first two are difficult to define quantitatively; however, qualitatively, it is well known (10) that geometric dispersion is most pronounced at wavelengths about equal to the cross-section dimensions of the propagation medium. The table below compares the wavelengths at 100 kHz for longitudinal waves in the three materials making up the path. Geometric dispersion in the propellant should be small, although dispersion due to propagation through the heterogeneous material containing AP particles comparable in size to emission wavelengths will be larger.

Material	$E(MN/m^2)$	c_o(m/s)	c_s(m/s)	λ_s(cm)
MC-XXX	2.75	38.4	22.3	.022
Alum.	68.7×10^3	5120	2970	2.97
Steel	206.2×10^3	5151	2987	2.99

$c_o \doteq \sqrt{E/\rho}$, c_s = Rayleigh speed $\approx 0.58\ c_o$

Attenuation due to acoustic impedance mismatch will occur at the propellant-holder, the holder-endplate, and the endplate-transducer interfaces (Figure 3). To a first approximation the overall attenuation

for complex waves may be represented as:

$$\text{Attenuation} = \frac{2}{1 + \frac{\rho_2 c_2}{\rho_1 c_1}}$$

where ρ = density, c = wavespeed, and propagation is from 1 to 2. For the present configuration, the net attenuation is approximately 0.0026 so that less than 1% of the energy at the source will arrive at the transducer element.

Several mechanisms have been considered as potential sources for the measured emissions. They can be broadly grouped as:

(a) solid phase effects such as dislocation kinetics or crystal fracture,

(b) gas phase phenomena such as ignition transients or combustion kinetics.

Since for these tests, energy has been increased over a 50 kHz to 300 kHz band, the sources can be further grouped according to characteristic frequencies. Solid phase effects are commonly observed as sources for acoustic emissions in materials tests, and it is generally agreed that a combination of dislocation movement and micro-fracture are prime amongst these. However, the characteristic times are in the sub-micro-second range so that the major energy release would occur well above the present band (and outside the range of all but the most exotic equipment). Furthermore, should this energy excite individual particles to vibrate, the characteristic frequencies (AP particles, for example) would again fall above 1MHz. Since definite peaks have been observed in the sub-300 kHz range, it must be concluded that other factors are

responsible.

Chemical kinetics times on the other hand are typically on the order of 10^{-5} seconds so that energy in the 100 kHz area can be anticipated. Three potential mechanisms were quantitatively explored and the conclusions summarized below:

(i) Laminar flame moving through a volume of fuel immediately above an AP particle: In this case, the acoustic pressure of interest is that across the flame as it propagates through the fuel. Using the momentum equation on this scale for a flame speed of roughly 1 cm/s yields an expected pressure fluctuation of about 2×10^{4} μ Bar. Considering only path attenuation this would produce a 50 μ Bar signal at the transducer.

(ii) AP ignition transient as the gas above a particle ignites. Here again the momentum equation can be crudely applied across the flame but now using the regression velocity rather than the laminar flame velocity above. For typical burn rates (1cm/s), the gas velocity normal to the surface can be estimated by mass conservation as about 100 cm/s. From the momentum equation, the pressure change will be roughly 100 times that above, or about 2×10^{6} μ Bar. This would produce a 5000 μ Bar signal at the transducer.

(iii) Explosive ignition of a fuel-oxidizer mixture near the surface. Considering typical specific heats for the fuel, a rough estimation yields gas velocities over 300 times the previous case. Accordingly, pressures in excess of 1 Bar would be seen at the transducer.

IV. Results

Burn Rate

The propellants were supplied by the Air Force Rocket Propulsion Laboratory and are shown in Table 1. Although no direct observation of burn rate was possible, the rate was determined from the onset and termination of the audible and ultrasonic signals. These burn rates for combustion in nitrogen are shown in Table 1 at the single pressure of 300 psia.

As may be seen from Table 1, the propellants are basically hydroxyl terminated polybutadiene - ammonium perchlorate (AP) - aluminum (Al) propellants with some additives. Parameter variations are systematically made in AP particulate size, aluminum coating (AFCAM), and catalyst.

In the test sequence, no reliable audible data were obtained for MC-174 and MC-175 because of the high burn rates. For these two propellants, steady state conditions were not achieved between the ignition and burnout transients. Data for MC-173 and MC-179 will be run in future tests to determine the effects of catalysts on the acoustic properties of the propellant. With the seven remaining propellants the effect of AP particulate size, aluminum coating, and aluminum addition can be studied. Also, the data are used to investigate the scaling laws presented in Section III. The combustion efficiency is presented along with the burn rates for those propellants for which reliable emission data were obtained. This efficiency is computed by integrating the audible spectrum over the range from 40 to 2000 Hz. Preliminary results for the spectrum from 2000 to 20 kHz indicate that most of the noise is produced at frequencies above 2000 Hz where

Table 1. PROPELLANTS FOR ACOUSTIC TESTING, AND BURN RATES AT 300 PSIA IN NITROGEN

Specimen	R-45M	AP		AL	Dioctyl dipate	Indopol	IPDI	Catalysts	Burn rate (in/sec)	$P/\dot{m}$ $(cm/sec)^2$
		Size	%							
MC-170	9.31%	200μ 14μ 6μ	26.8 20.4 20.8	20% 5μ		2.0%	0.69%		0.31 ±0.3	.65
MC-172	9.31%	200μ 14μ 6μ	26.8 20.4 20.8	20% 5μ AFCAM		2.0%	0.69%		0.37 ±0.01	.55
MC-173	9.31%	200μ 14μ 6μ	26.8 20.4 18.8	20% 5μ	2%		0.69%	Fe_2O_3 2%	0.52	-
MC-179	9.31%	200μ 14μ 6μ	26.8 20.4 18.8	20% 5μ	2%		0.69%	Copper fluoride 2%	Bad burn	-
MC-174	10.24%	6μ 0.5μ	26 40	20% 5μ		3.0%	0.76%		0.57	-
MC-175	10.24%	6μ 0.5μ	26 40	20% 5μ AFCAM		3.0%	0.76%		0.81	-
MC-177	9.31%	400μ 200μ 50μ	44 18 6	20% 5μ		2.0%	0.69%		0.21 ±0.02	.08
MC-178	9.31%	400μ 200μ 50μ	44 18 6	20% 5μ AFCAM		2.0%	0.69%		0.21 +0.03	Transducer Calibration Uncertain
NT-2	?	200μ	100%	NONE					.20±.01	1.2
NT-3	?	90μ	100%	NONE					.22±.02	1.3
NT-4	?	50μ	100%	NONE					.33±.03	2.5

transverse modes can exist in the tube. However, the tube characteristics above 2000 Hz will be thoroughly investigated before data at these higher audible frequencies are presented. The data from 40 to 2000 Hz is sufficient to show the effect propellant properties and to investigate scaling laws.

All tests were run with the propellants coated with about 1/4-inch of Dow Corning 140 RTV adhesive to prevent recirculating burning aluminum from igniting the sides of the propellant. Unless otherwise noted tests were run at 20 atm in nitrogen with 1/2 x 1/2 cm samples approximately eight cm in length.

Audible

According to Eq. (9), the total power of an equivalent open flame can be expected to increase directly with an increase in propellant area and to increase as the burn rate to the fourth power. From Eq. (9) the acoustic efficiency should scale like

$$\frac{P}{\dot{m}} \propto \frac{1}{\bar{c}} \left(\frac{\rho_s r}{\bar{\rho}} \right)^3 \qquad (11)$$

From Table 1, assuming $\bar{\rho}$, $\bar{c}$, and ρ_s are the same, the combustion noise efficiency for MC-170 and MC-177 should differ as $\left(\frac{r_{MC-170}}{r_{MC-177}} \right)^3$ or by a factor of from 2 to 6 for the burn rates measured. The measured difference of about a factor of 8 is not unreasonable. Similarly the difference in $P/\dot{m}$ for NT-2 and NT-4 bears out Eq. (11) to within experimental error. From the data obtained thus far, Eq. (11) is in qualitative agreement with experimental data.

The scaling of Eq. (9) with respect to area has been investigated in this study and in Ref. 3. The results indicate that, to within 20%, the measured power is linearly proportional to the propellant area.

For the aluminized propellants, the effects of propellant properties and pressurization gas on the measured spectra are presented in Fig. 4. Comparison of the curves for MC-177 burned in air and nitrogen indicates a 10 to 15 db rise in sound power level for the run with air. The difference in the results appears to be caused by aluminum afterburning. The effect of an AFCAM coating can be observed from comparison of the spectra for MC-170 and 172. The propellant without AFCAM appears to have a slightly higher noise output over the frequency range from 200 to 2000 Hz.

Shown on Fig. 4 are the burn-through frequencies computed from Eq. (10) using the MC-170 burn rate for various AP and Al particle sizes. Because of variations in granularity, it is seen that the spectrum is rather densely occupied by available frequencies. No apparent correlation of the observed spectra with these frequencies is evident; none was really expected to be clear because of the roughness of the estimate of frequency, the usual spread of particle size about the stated value and the dense population of the spectrum with these particle frequencies. Nevertheless, moving from MC177 to MC170 propellant, which decreases the mean particle size and increases the burn rate (see Table 1), there is a general rise in the spectrum and a filling of the spectrum in the frequency range from 350 to 1000 Hz (perhaps due to the 14 μ AP). In the 5 μ range between 1000 and 2000 Hz the spectra for the aluminumized propellants are consistently flat and the sound power level is the lowest.

In contrast to the aluminized propellants, the spectra for the non-aluminized propellants, shown in Fig. 5, indicate a general increase in noise with decreasing particle size over the 1000-2000 Hz range. Comparison of the curves show a general increase in the sound levels from 300 to

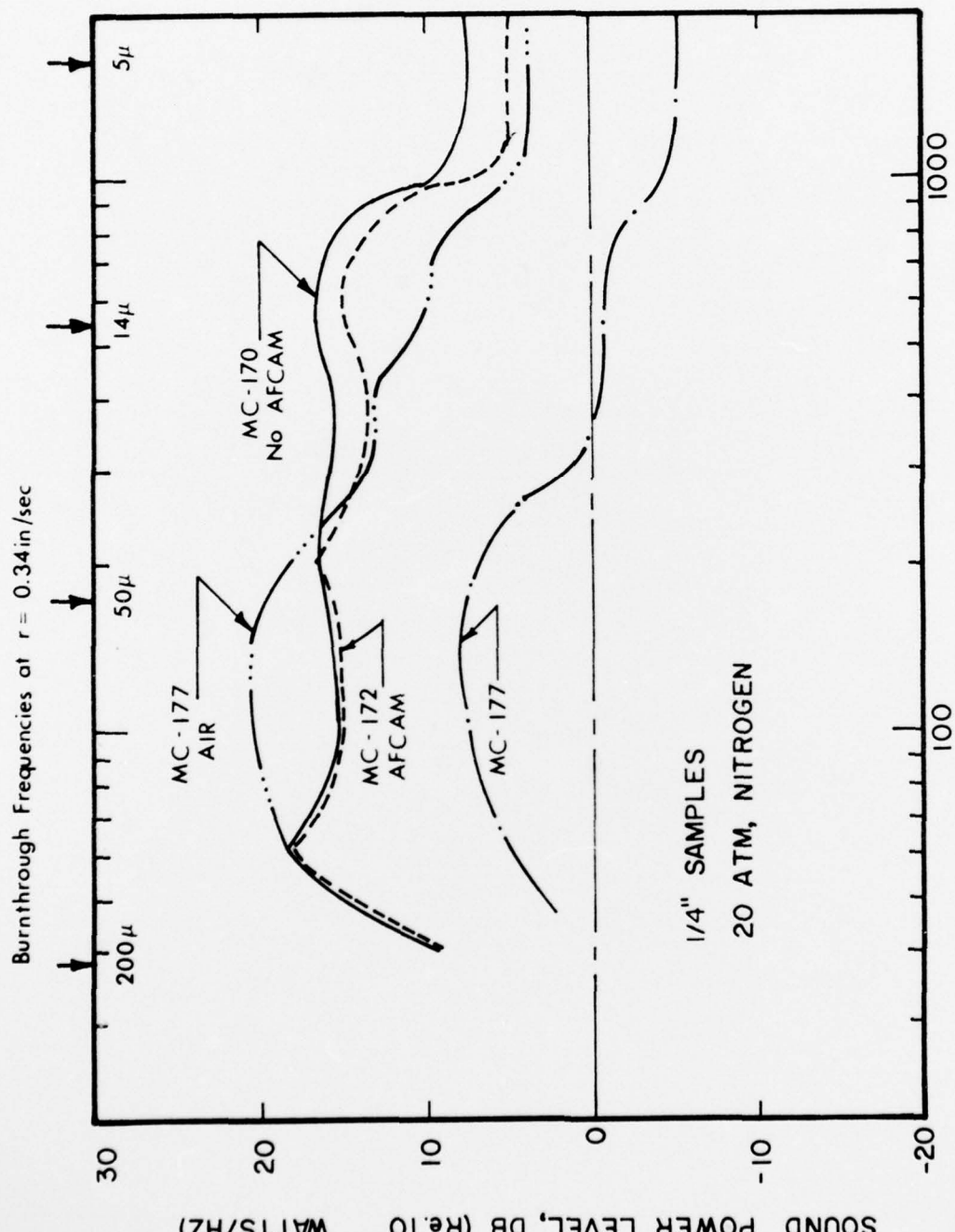

FIGURE 4. EFFECT OF AP PARTICLE SIZE, AFCAM TREATMENT, AND GAS MEDIUM ON DEDUCED FREE FIELD SPECTRA.

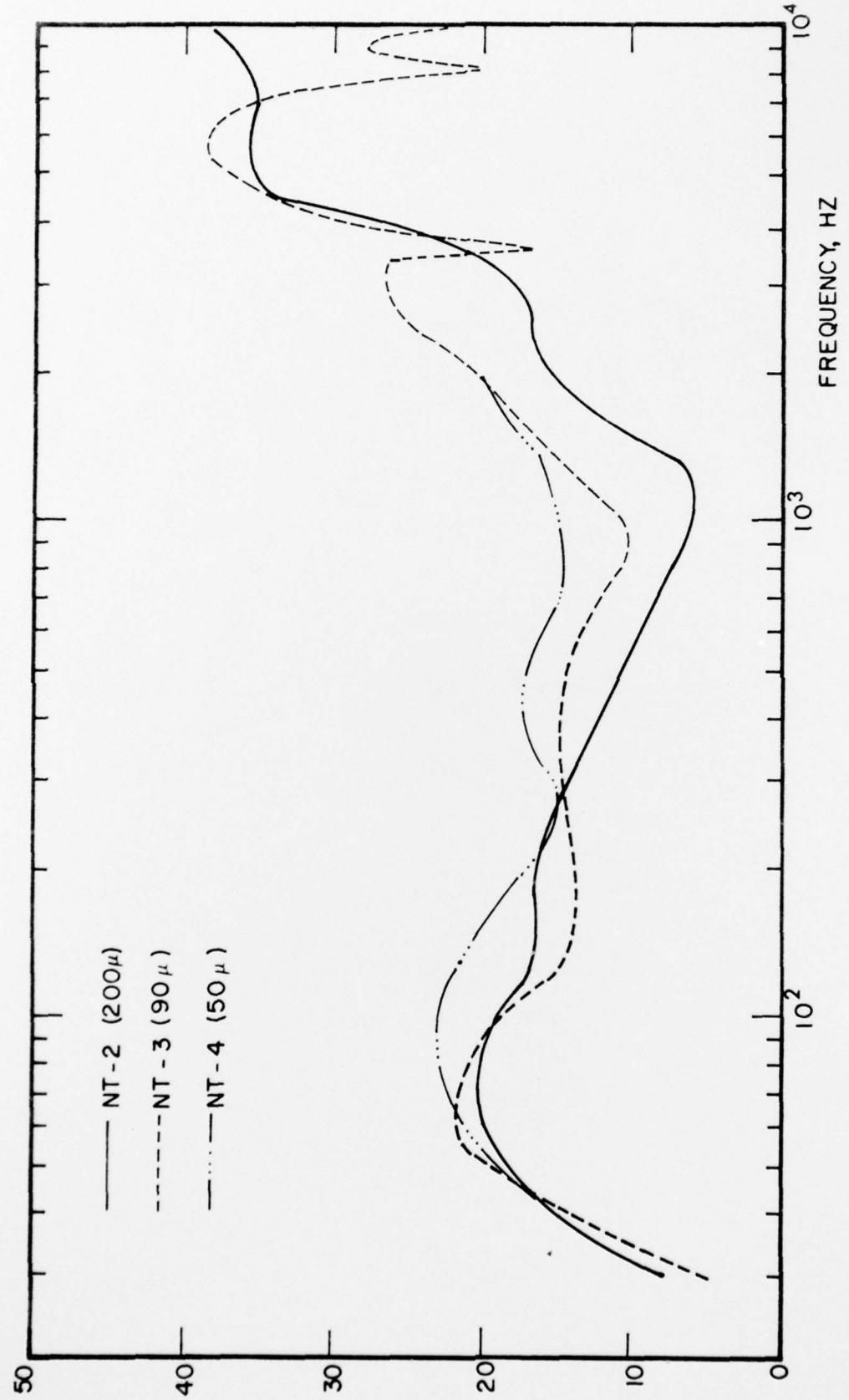

FIGURE 5. COMPARISON OF DEDUCED FREE FIELD SPECTRA FOR NONALUMINIZED PROPELLANTS BURNED AT 300 PSIA IN NITROGEN.

2000 Hz probably caused by the higher burn rate of NT-4 as mentioned previously. Below 300 Hz no general trend can be ascertained. From 2 to 10 kHz there is a 10 to 20 db rise in sound power level over the noise measured below 2000 Hz. Using Eq. (10) this noise is produced by sources on the order of one micron which is of the same order as the reacting surface layer. Including the noise over this frequency range increases the values of $P/\dot{m}$ computed from 0 to 2000 Hz by three orders of magnitude and may explain the observed roughness levels in rocket motors. An investigation is currently underway to check the accuracy of the assumption that the propellant noise output can be approximated by a point source given in Eq. (2). If these preliminary data are valid, the majority of the audible combustion noise falls within the 2000 to 10,000 Hz range.

Ultrasonic

Ultrasonic acoustic emission data were obtained for all propellants in Table 1 except MC-173 and MC-179. The effect of the following variables on the spectral data are presented. (1) AP particle size, (2) pressurization gas, (3) aluminum particles, and (4) AFCAM coating. Details of the data reduction methods are given in Ref. 3 .

AP Particle Size: For the nonaluminized propellants-NT-2, NT-3, and NT-4-AP particle size has little effect on either the overall sound power level or the location of the peaks in the spectrum. Based on these data no correlation appears to exist between the spectral peaks and the particle size as shown in Fig. 6.

Effect of Pressurization Gas: The burning of MC-177 in air as opposed to nitrogen produces a definite shift in both spectral peaks and peak

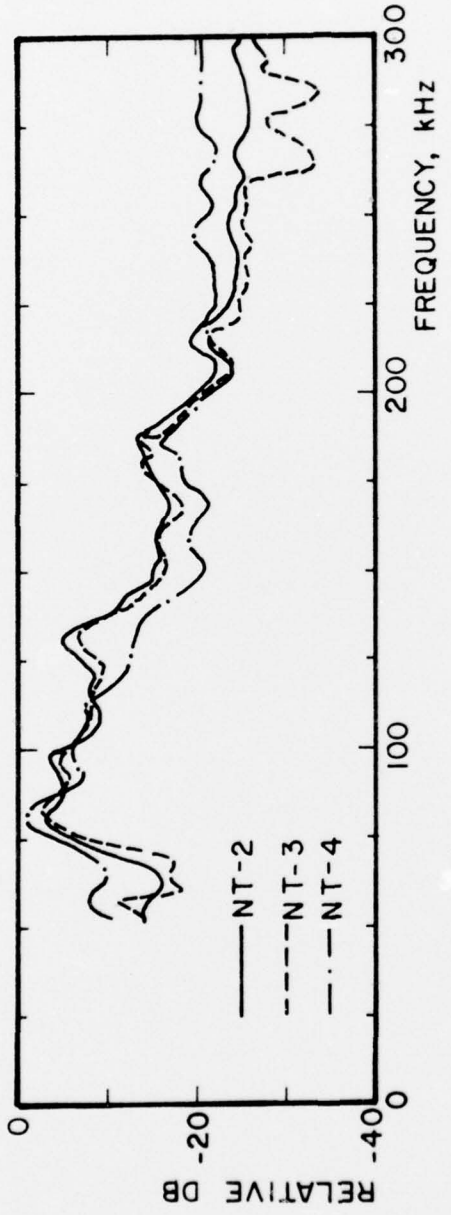

FIGURE 6. EFFECT OF AP PARTICLE SIZE ON THE ACOUSTIC EMISSION SPECTRA FOR NONALUMINIZED PROPELLANTS BURNED IN NITROGEN AT 300 PSIA.

power as shown in Fig. 7. In air there is a stronger high frequency content than in nitrogen. There is also a general smoothing of the spectra for air at the frequencies below 125 kHz. These effects are most probably caused by aluminum afterburning although correlation between the spectral peaks and the combustion process is presently not clear.

Aluminum Particle Addition: As shown in Fig. 6, AP particle size does not have a pronounced effect on the spectra of the acoustic emissions. However, the addition of aluminum does. Comparison of the spectra for aluminized (MC-177) and nonaluminized (NT-2) propellants indicate markedly different spectral features. The spectrum of the aluminumized propellant has a large noise content at the low frequency range below 125 kHz. Also, the peaks in the aluminized propellant spectrum are more distinct in the 125 to 225 kHz range. Above 225 kHz, however, relatively little difference is apparent in the two spectra in Fig. 8. Whether the cause of the differences is the emission source or propagation of the ultrasonic waves through the propellant cannot be ascertained.

Effect of AFCAM Coating: As reported in Ref. 3 there was a general increase in overall sound power when the aluminum is coated with AFCAM for MC-177 and MC-178. This trend also holds for MC-170 and MC-172 as shown in Fig. 9.

Source Characteristics: Based on the earlier observations reported in Ref. 3, it was strongly suspected that the AP deflagration mechanism was primarily responsible for the observed emission spectra. The considerations summarized in Section III of the present report provide a crude

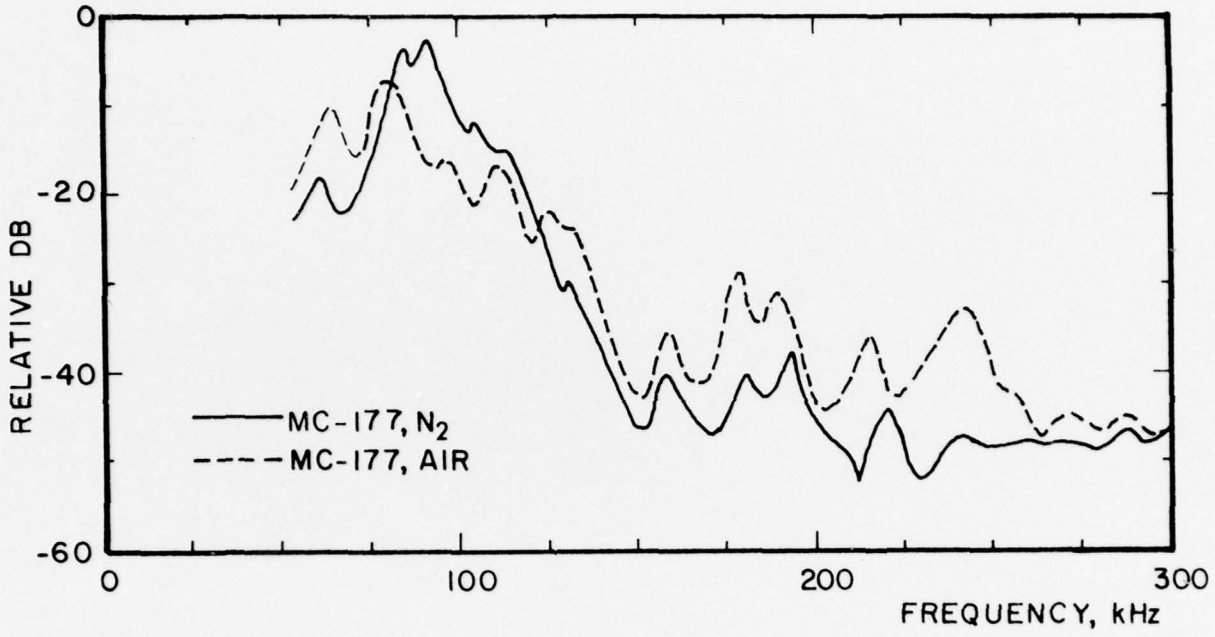

FIGURE 7. EFFECT OF PRESSURIZATION GAS ON THE ULTRASONIC SPECTRA OF MC-177 AT 300 PSIA

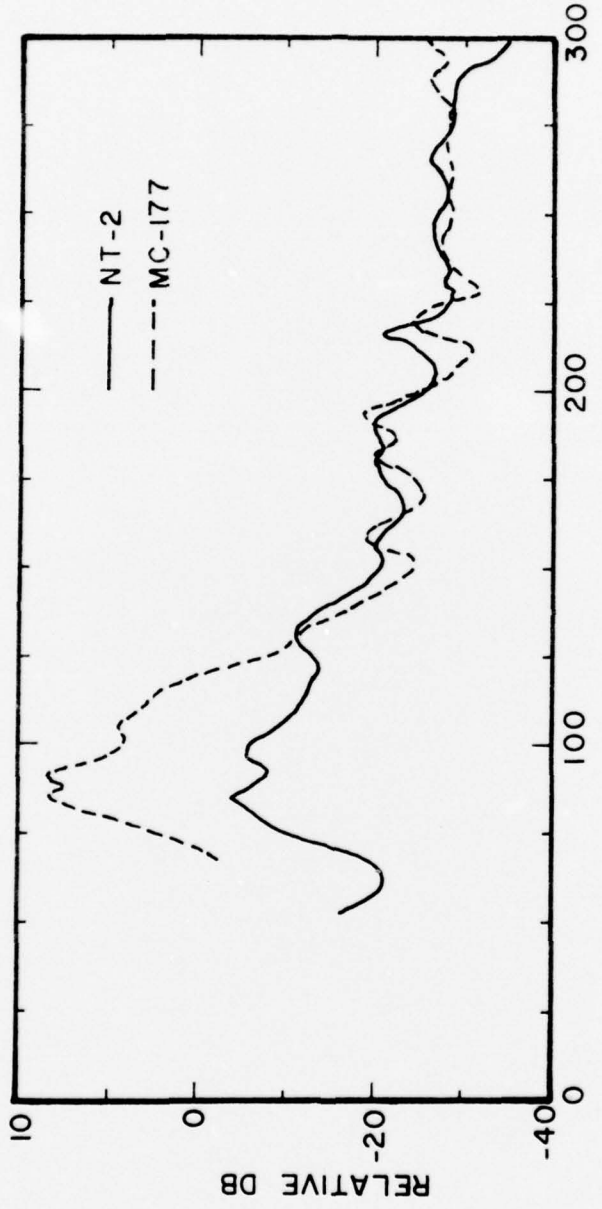

FIGURE 8. EFFECT OF ALUMINUM ADDITION ON THE ULTRASONIC SPECTRA AT 300 PSIA BURNED IN NITROGEN.

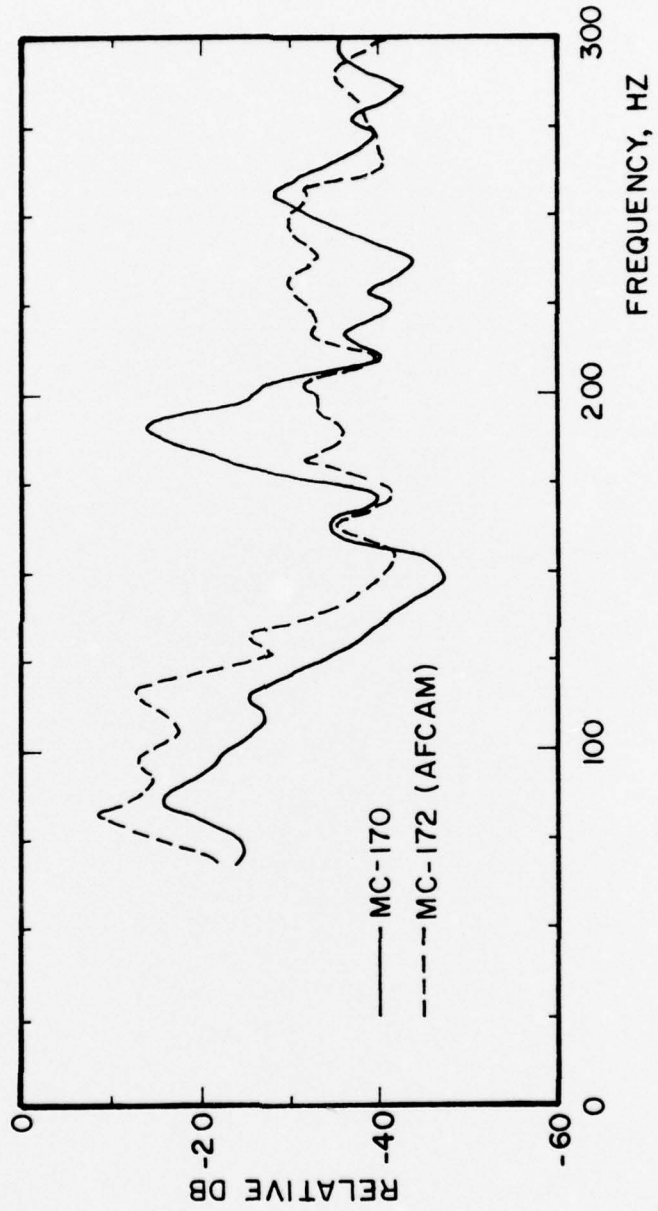

FIGURE 9. EFFECT OF AFCAM COATING OF THE ALUMINUM PARTICLES AT 300 PSIA IN NITROGEN.

theoretical basis for this hypothesis as well. The rms acoustic emission levels at the transducer consistently range between about 800 to 3500 Bar. These levels are somewhat above the range for the laminar flame model, (i), but are generally consistent with the AP ignition transient model, (ii). The chemical kinetics times associated with both of these processes are on the order of 10^{-5} sec so that the accompanying unsteady pressures would be expected to show relatively larger spectral energy content near 100 kHz. Again, this is consistent with the earlier observations of a large, 15 - 25 dB, peak in the emission power spectra around 100 kHz. Furthermore, since these characteristic times should be only weakly affected by pressure and unaffected by AP size, the principal alteration in the emission spectra should be a change in the relative height of the 100 kHz peak as AP sizes and burn rates are varied. In this case, the change in level is associated with the changing source areas.

Unfortunately, as shown in Figure 6, there is no clear difference in the shape or level of the emission spectra as the AP size is varied from 50 m to 200 m (NT series). The spectra show some fine structure but are basically flat within the tolerances of the calibration curve used. On the other hand, as shown in Figure 8, it is much more likely that the observed peak at 100 kHz can be attributed to the Al present in the more complex MC propellants. This possibility has not yet been fully explored in tests to date, although several comments might be made. From the levels involved, the signals would likely be produced before the Al agglomerates have left the burning surface (there is some indication, however, that the peak may be due to Al particle impact on the inner

tube walls). Emissions from the solid phase Al due to dislocation activity or micro-fracture are well above the 100 kHz range. Propellants with a range of Al sizes and quantities will have to be tested in order to further clarify these observations. For example, insensitivity to Al size could indicate a source mechanism associated with the agglomerate phase.

V. Conclusions

There is a marked effect of pressurization gas on the audible and ultrasonic emission. The audible spectra shows a 10 db increase in sound power level. No distinct differences in spectral shape are apparent between two propellants of different AP particle size. However, the audible spectra do indicate an increase in overall power output with a decrease in AP particle size probably caused by the increasing burn rate with decreasing particle size.

The theory presented in Ref. 3 adequately describes the behavior of the audible noise output in the range of frequency from 0 to 2000 Hz. This theory assumes that the mechanism of the noise is a velocity source caused by the heterogeneity of the propellant. Above 2000 Hz the wave characteristics of the tube must be better understood before comparison between the theory and experiment is made.

In contrast to Ref. 3 , the effect of aluminum coating (AFCAM) on the audible noise is not significant when burning in nitrogen. However, there is a general increase in the ultrasonic emissions when AFCAM is used.

VI. Nomenclature

A	combustion noise source strength
A_p	propellant surface area
c	speed of sound
f	frequency of maximum radiated sound power
h	combustion noise monopole source strength
k	wavenumber, $\omega/\bar{c}$
ℓ	tube length
ℓ_e	mean granularity distance
$\dot{m}$	mass flow of propellant
p	acoustic pressure
$\bar{p}$	mean chamber pressure
r	radical distance or burn rate
R	distance from the source
S	tube cross-section area
S_ω	power spectral density (PSD)
t_o	sampling time of Fourier transform
X	axial distance
$<>$	time average
α	95% confidence limits for PSD
γ	ratio of specific heats
δ	Dirac delta function
ζ	specific acoustic impedance
ρ	density
η	mass flow noise efficiency, $P/\dot{m}$
θ	tangential coordinate

Subscripts

ℓ at tube length

ω Fourier transform

s solid phase

r real part

i imaginary part

Superscripts

* Complex conjugate

- Steady State Values

VII. References

1. Saber, A. J., Johnston, M. D., Caveny, L. H., Summerfield, M., and Koury, J., "Acoustic Emissions from Burning Solid Propellant Strands," 11th JANNAF Combustion Meeting, CPIA Publication No. 261, December 1974, pp. 409-428.

2. Caveny, L. H., Saber, A. J., and Summerfield, M., "Propellant Combustion and Burning Rate Uniformity Identified by Ultrasonic Acoustic Emissions," AIAA Paper No. 76-696, Presented at the AIAA/SAE 12th Propulsion Conference, Palo Alto, Calif., July 1976.

3. Craig, J. I., Strahle, W. C., and Palfrey, J., "Audible and Ultrasonic Acoustic Emissions from Composite Solid Propellants," AFOSR Interim Scientific Report for Grant No. AFOSR-75-2805, July 1975.

4. Morse, P. M. and Ingard, K. U., Theoretical Acoustics, Mc-Graw Hill, New York, 1964, Chapter 9.

5. Strahle, W. C., "Some Results in Combustion Generated Noise," Journal of Sound and Vibration, 23, 113-125, 1972.

6. Strahle, W. C. and Shivashankara, B. N., "A Rational Correlation of Combustion Noise Results from Open Turbulent Premixed Flames," Fifteenth Symposium (International) on Combustion, The Combustion Institute, Pittsburgh, 1974, pp. 1379-1385.

7. Bell, R. L., "Acoustic Emission Transducer Calibration-Transient Pulse Method," Tech Report DE-73-3, Dunegan-Endevco, San Juan Capistrano, California, 1973.

8. Cady, W. G., Piezoelectricity, McGraw-Hill, New York, 1946.

9. Hill, R. and Stephens, R. W. B., "Acoustic Emission-Evaluation of Transducers and Measuring Systems", Proceedings of the Ultrasonics International 1973 Conference, 5.5, pp. 177-182.

10. Kolsky, H., Stress Waves in Solids, Oxford: University Press, 1953.